Supplement: Whole-lithosphere shear during oblique rifting

[1]Lutz, Brandon M., [1]Axen, Gary A., [1]van Wijk, Jolante, [1]Phillips, Fred M.

[1]Earth and Environmental Science Department, New Mexico Institute of Mining and Technology,

801 Leroy Pl, Socorro, NM 87801

CONTENTS

LIST OF FIGURES and TABLES

A. DESCRIPTION OF GPLATES KINEMATIC RECONSTRUCTION

Lutz (2021) reconstructed extension in the central Basin and Range using three main reconstruction paths that relate fault block kinematics to relative Euler pole rotations (Fig. S1 and Tables S1-S3). The main reconstruction path links the Sierra Nevada to the Colorado Plateau through the center of the Death Valley region (black in Fig. S1 and Table S1). The northeastern reconstruction (blue in Fig. S1) path relates fault block kinematics northeast of the Furnace Creek fault zone (FCFZ) (e.g. Silver Peak Range to Funeral Mountains) to the main reconstruction path via the Resting Spring Range (Table S2). The southern reconstruction path (green in Fig. S1) involves the Argus Mountains, Slate Range, and Granite Mountains south of the Garlock fault (Table S3). This path links to the main path via the Panamint Mountains.

Here we simply present tables of Eueler pole rotations that drive the kinematic model. The relative motions between crustal fault blocks from which the rotations are derived can be found in Lutz (2021).

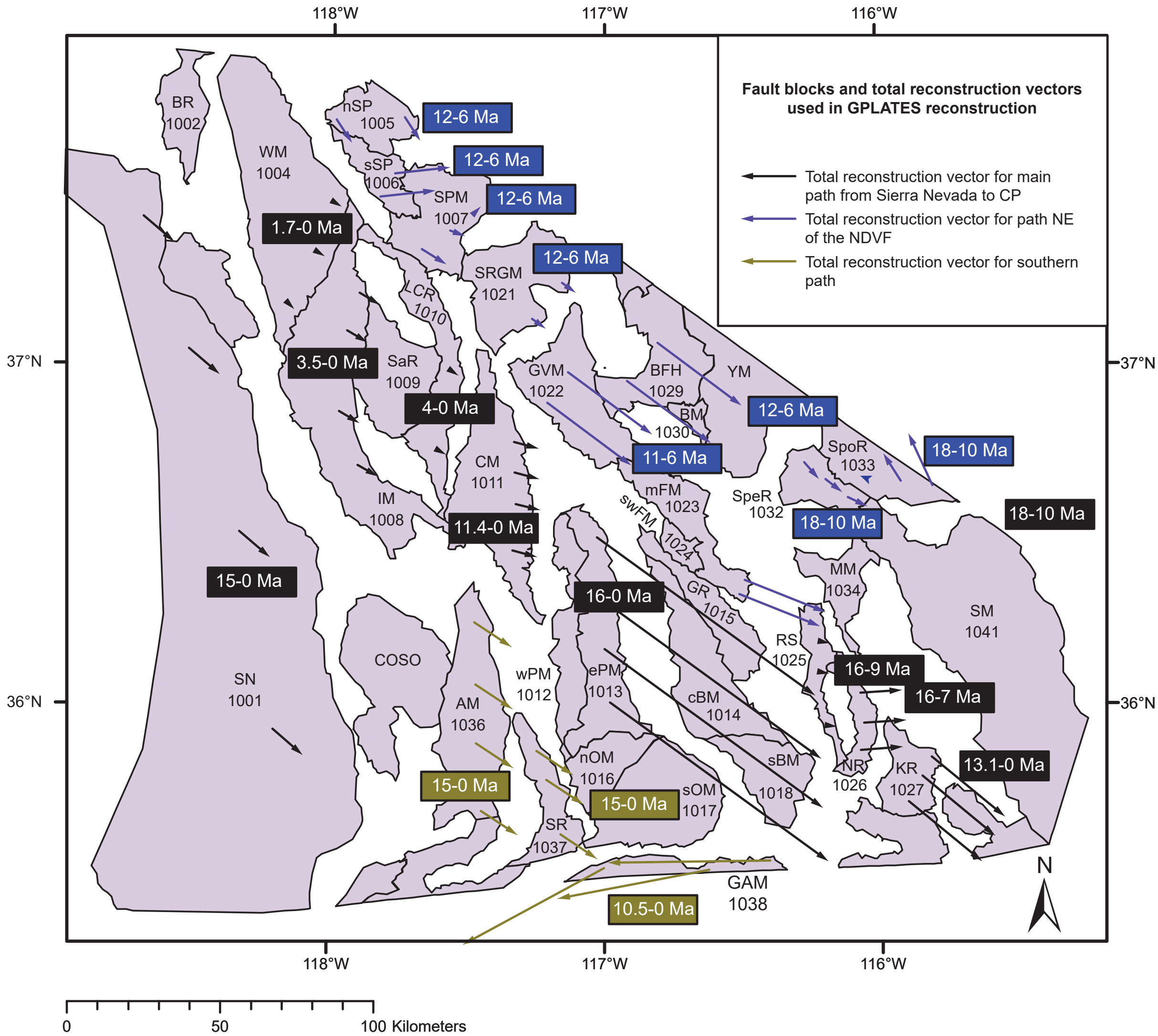

Figure S1. Map of the Death Valley region showing total reconstruction vectors between major fault blocks. Mountains and ranges associated with the numbers shown in range blocks are given in Tables S1-S3 and are separated out as sections in the Supplemental Material text. Abbreviations for mountains (fault blocks): AM: Argus Mountains. BFH: Bullforg Hills. c/sBM: Central/S Black Mountains. BM: Bare Mountain. BR: Benton Range. CM: Cottonwood Mountains. COSO: Coso Range. m/swFM: Main/SW Funeral Mountains. GAM: Granite-Avawatz Mountains. GR: Greenwater Range. GVM: Grapevine Mountains. IM: Inyo Mountains. KR: Kingston Range. LCR: Last Chance Range. MM: Montgomery Mountains. NR: Nopah Range. n/sOM: N/S Owlshead Mountains. E/W Panamint Mountains. RS: Resting Spring Range. SaR: Saline Range. SM: Spring Mountains. SN: Sierra Nevada. n/sSP: N/S Silver Peak Range. SpeR/Specter Range. SpoR: Spotted Range. SPM: Sylvania-Palmetto Mountains. SR: Slate Range. SRGM: Slate Range-Gold Mountains. e/wPM: YM: Yucca Mountain. WM: White Mountains.

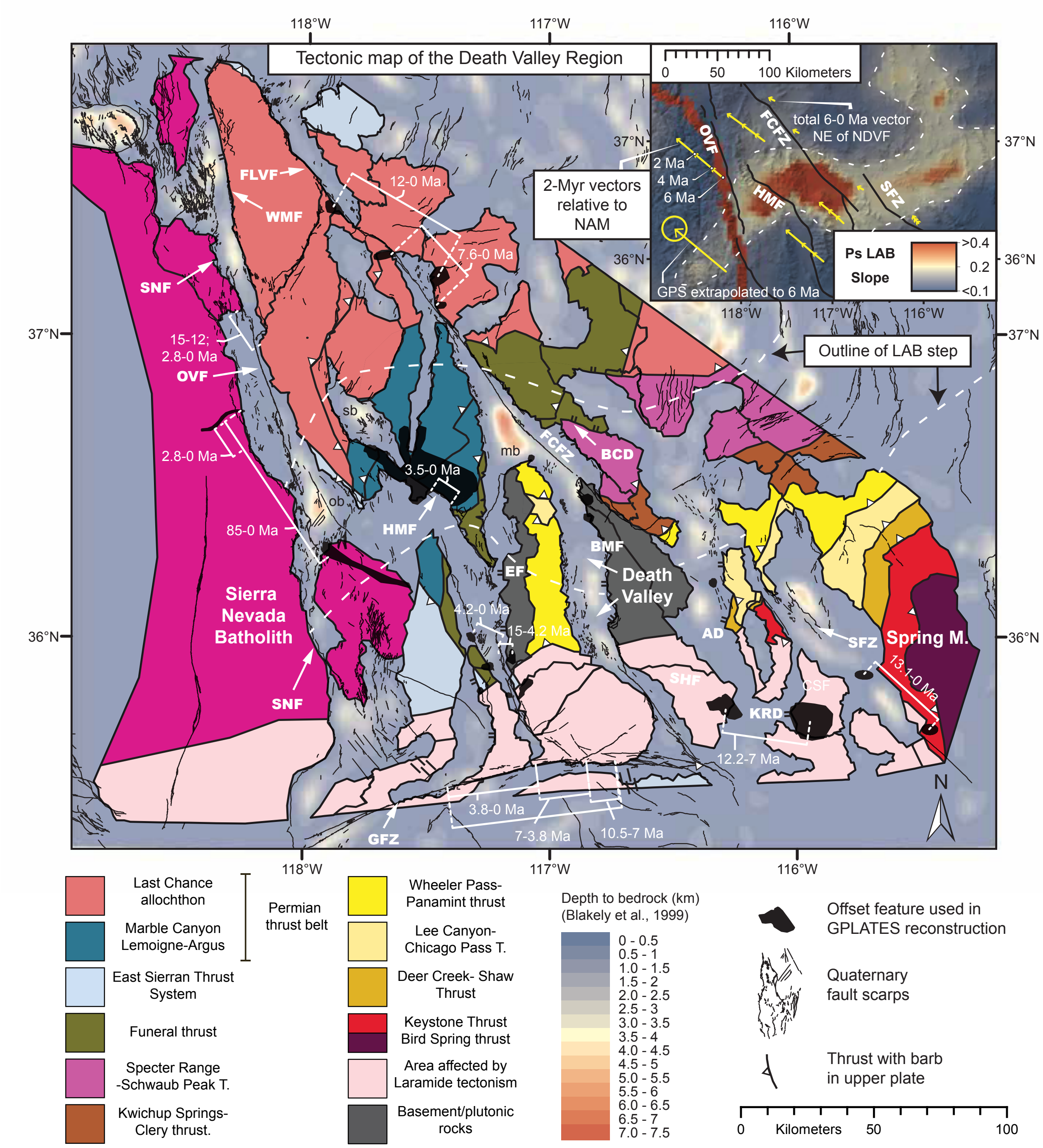

Figure S2. Map of the Death Valley region showing Quaternary faults, thrust plates, basin thicknesses, offset features, and the LAB-depth gradient (dashed white lines and color map on top right). Thrust plate map after Lutz et al. (2021). AD: breakaway of Amargosa Detachment. BCD: Boundary Canyon detachment. BMF: Black Mountains fault zone. CSF: Crystal Springs fault zone. EF: Emigrant fault. FLVF: Fish Lake Valley fault. GFZ: Garlock fault zone. HMF: Hunter Mountain fault zone. KRD: Kingston Range detachment. OVF: Owens Valley fault zone. SHF: Sheephead fault zone. SNF: Sierra Nevada frontal fault zone. SFZ: Stateline fault zone. WMF: White Mountains fault zone.

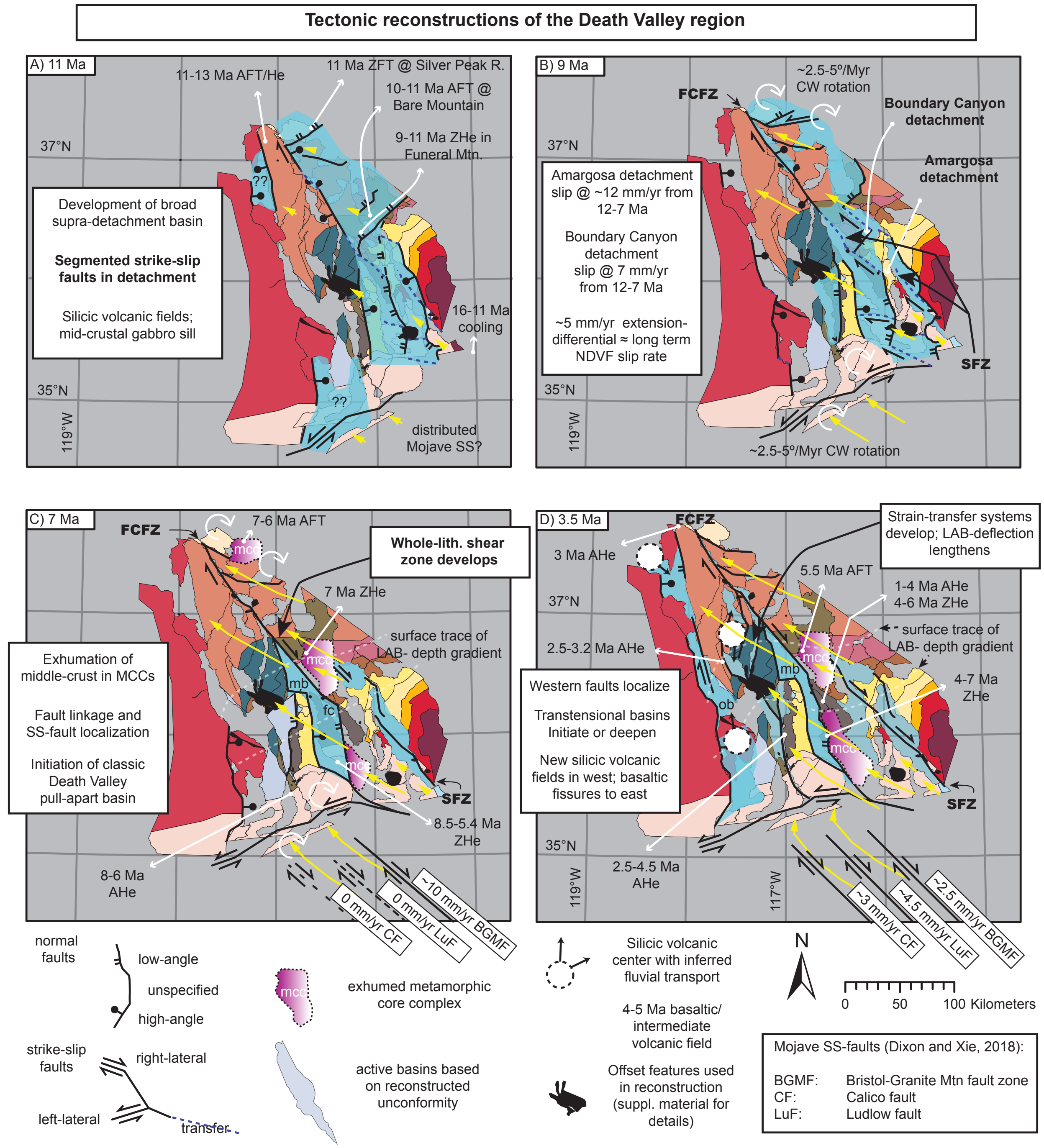

Figure S3. Reconstructions of the DVR at selected times. See Fig. S2 for the thrust plates and abbreviations. See animation for a full reconstruction sequence in 0.1-Myr time-steps. Note the evolution of the LAB depth gradient deflection in C and D (dashed white line).

Table S1

Euler Pole rotations and kinematic inputs for the main reconstruction path

Fault Block Restoration	Time (Ma)	Longitude (°)	Latitude (°)	Angle (°)	Kinematic inputs and notes	References
Sierra Nevada-White (1001-1004)	0	90.0000	0.0000	0.0000	11.1 km of post-2.8 Ma separation (322°) on Owens Valley fault; yields ~3.4-3.7 mm/yr slip rate, consistent with paleo-seismic and GPS-based slip-rate models; 3 km 15-12 Ma separation on White M fz	(Bachman, 1978; Lee et al., 2001b; Stockli et al., 2003; Kirby et al., 2008)
	2.8	29.9617	-2.6572	0.0994		
	12	29.9617	-2.6572	0.0994		
	15	37.8448	7.3692	0.1185		
Benton-White (WM) (1002-1004)	0	90.0000	0.0000	0.0000	7.5 km of 3-0 Ma NW-separation on White Mtns fz based on gravity-based basin depth	(Lutz, 2021)
	3	47.3236	28.3724	0.0670		
White-Inyo (1004-1008)	0	3.0531	-25.7158	0.0000	1.1 km of post-1.7 Ma separation (306°) on Deep Springs fault	(Lee et al., 2001a)
	1.7	44.5760	20.3368	0.0093		
Inyo-Last Chance (1008-1010)	0	90.0000	0.0000	0.0000	8.2 km of 3.5-0 Ma NW-separation on the normal faults in the Saline Range linked to dextral slip on the Hunter Mountain fz	(Burchfiel et al., 1987; Sternlof, 1988; Oswald and Wesnousky, 2002; Lee et al., 2009; Knott et al., 2019)
	3.5	43.8131	17.8028	0.0730		
Last Chance-Cottonwood (1010-1011)	0	90.0000	0.0000	0.0000	2 km of post-4 Ma separation (301°) on the Tin Mountain fz	(Snow and White, 1990; Knott et al., 2019)
	4	42.7356	16.1162	0.0183		
Cottonwood-wPanamint (1011-1012)	0.0	90.0000	0.0000	0.0000	2.5 km of 3-4.2 Ma NW-separation on the Towne Pass fault zone; the 7.6 Ma rotation is to align the offset granitic stocks along the FCFZ; 5.7 km of 7.6-11.4 Ma slip to get to the 8.5 km of total Miocene-recent Cottonwood-Panamint Mountains separation.	(Hall, 1971; Hodges et al., 1989; Snyder and Hodges, 2000; Andrew and Walker, 2009; Nachbor and Wetmore, 2017)
	3.0	22.0385	-10.7998	0.0004		
	4.2	42.5509	15.7942	0.0236		
	7.6	51.6544	42.2697	0.0552		
	11.4	51.1336	39.4012	0.0758		
ePanamint-Resting Spring (1013-1025)	1.2	31.9479	0.6385	0.0373	4.05 km of post-1.2 Ma offset from basaltic gravels; 3.95 km offset of gravels from 3.3-1.2 Ma; yields 3.5 mm/yr for FCFZ; Closure of central DV graben at 7 Ma; ~40 km of post-7.6 Ma offset from granitic stock along FCFZ; 45 km of post-12 Ma NW-separation on Jurassic batholiths across FCFZ; 7.5 km of 16-12 Ma E-W extension based on thrust plate correlations	(Stewart, 1983; Oakes, 1987; Reheis and Sawyer, 1997b; Klinger and Sarna-Wojcicki, 2001; Frankel et al., 2007; Renik and Christie-Blick, 2013; Bidgoli et al., 2015)
	3.3	31.8906	0.5727	0.0714		
	7	26.7826	-5.0154	0.1260		
	7.6	31.8855	0.6439	0.2997		
	12	38.9975	9.9071	0.7314		
	16	40.4581	12.2462	0.7912		
nOwlshead-ePanamint (1016-1013)	0	90.0000	0.0000	0.0000	Estimated 26° of post-14 Ma clockwise vertical-axis rotation from alignment of Wingate Wash fault to Amargosa detachment; offset magnetic anomalies	(Guest et al., 2003; Luckow et al., 2005; Fridrich and Thompson, 2011)
	14	35.9121	116.9886	19.4077		
Resting Spring-Nopah (1025-1026)	0	90.0000	0.0000	0.0000	~5 km of 16-9 Ma WSW-directed separation based on syntectonic Miocene deposits and ca. 9 Ma volcanics deposited on tilted Resting Spring Rng	(Snow and Wernicke, 2000; Niemi et al., 2001; Fridrich and Thompson, 2011)
	9	90.0000	0.0000	0.0000		
	16	53.0142	49.6767	0.0267		
Nopah-Kingston (1026-1027)	0	90.0000	0.0000	0.0000	~14 km of total 16-7 Ma separation based on thrust plate correlations; 9 km (273°) from 16-13.5 Ma and 5 km (242°) from 13.5-7 Ma; 13.5-7 Ma separation based on offset tuff and inferred cessation of slip on the Crystal Springs fz	(Topping, 1993; Davis et al., 1993; Workman et al., 2003; Fridrich and Thompson, 2011; Lutz et al., 2021)
	7	90.0000	0.0000	0.0000		
	12	45.5546	104.8543	0.0302		
	16	53.6392	70.1319	0.1220		
Kingston-Spring (1027-1041)	0	90.0000	0.0000	0.0000	~30 km of total separation (309°) on Stateline fz since 13.1 Ma, with most slip prior to 3.5 Ma; post-3.5 Ma slip rate of 0.8 mm/yr, consistent with GPS-based models	(Burchfiel et al., 1983; Wernicke, 2004; Hill and Blewitt, 2006; Guest et al., 2007; Fridrich and Thompson, 2011)
	3.5	38.7400	9.7501	0.0273		
	13.1	38.0834	8.8208	0.2809		
sBlack-Black (1018-1014)	0	90.0000	0.0000	0.0000	~25 km separation between Sperry Hills granite megabreccia and Kingston Range pluton; includes 16.7° of CW vertical axis rotation; setup yields ~20 km separation on the Sheephead fault	(Topping, 1993; Renik, 2010; Fridrich and Thompson, 2011; Flemming, 2018)
	7	36.2844	116.0559	0.0709		
	12.2	36.3881	115.7466	16.7400		
Spring-Colorado Plateau (1041-101)	0	90.0000	0.0000	0.0000	~47 km of 15-11 Ma WSW-separation on Las Vegas Valley shear zone, ~65 km of 16-12 Ma separation between Frenchman Mtn and CP based on megabreccia and reconstruction of Virgin Mtns detachment; ~ 54 km of 16-12 Ma extension between Mormon Mtns and CP based on cross-section reconstruction through Beaver Dam/Tule springs and Mormon Peak detachments	(Wernicke et al., 1988; Duebendorfer and Black, 1992; Axen, 1993; Duebendorfer et al., 1998; Snow and Wernicke, 2000)
	10	27.5230	102.2949	0.0032		
	12	53.5334	42.0763	0.1045		
	14	51.8565	87.6819	0.3874		
	16	51.7063	87.0002	0.7585		
	18	52.9948	78.5016	0.8668		

Table S2

Euler Pole rotations and kinematic inputs for the northern reconstruction path

Fault Block Restoration	Time (Ma)	Longitude (°)	Latitude (°)	Angle (°)	Kinematic inputs and notes	References
nSilver Peak-sSilv Peak (1005-1006)	0	90	0	0.0000	~9.3 km of 12-6 Ma left-lateral oblique-normal separation, part of the total 20-30 km separation on the Silver Peak-Lone Mtn detachment system	(Stewart and Diamond, 1990; Oldow et al., 1994; Petronis et al., 2002a; Petronis et al., 2007; Oldow et al., 2009; Petronis et al., 2009; Mueller, 2019)
	6	90.0000	0.0000	0.0000		
	12	25.8348	-5.8675	0.0840		
sSilver Peak-Sylvania/Palmetto (1006-1007)	0	90.0000	0.0000	0.0000	~18 km of 12-6 Ma left-lateral oblique-normal separation, part of the total 20-30 km separation on the Silver Peak-Lone Mtn detachment system	
	6	90.0000	0.0000	0.0000		
	12	51.8797	72.6145	0.1659		
Sylvania/Palmetto-Slate/Gold (1006-1007)	0	90.0000	0.0000	0.0000	25° CW rotation from 12-6 Ma based on paleomagnetic, thermochronology and geochronology around the Silver Peak-Lone Mtn detachment system.	
	6	90.0000	0.0000	0.0000		
	12	37.4937	117.4980	25.0952		
Slate/Gold-Grapevine (1021-1022)	0	90.0000	0.0000	0.0000	5.5 km of 12-6 Ma normal-sense separation (306°); yields 0.9 mm/yr extension rate across Bonnie-Claire flat, consistent with very low Quaternary slip rates nearby	(Machette et al., 2004; Hoeft and Frankel, 2010; Foy et al., 2012; Lifton et al., 2015)
	6	90.0000	0.0000	0.0000		
	12	40.3499	12.6587	0.0498		
Grapevine-mainFuneral (1022-1023)	0	90.0000	0.0000	0.0000	35 km of 12-7 Ma normal-sense separation (306°) along the Boundary Canyon detachment based on offset Eocene-early Miocene normal faults, correlation of tectonic mélange, thermo-chronometry, thermo-kinematic modeling	(Hoisch and Simpson, 1993; Applegate and Hodges, 1995; Snow and Wernicke, 2000; Beyene, 2011)
	7	36.4318	-12.6568	-0.0003		
	12	39.8758	11.6323	0.3151		
swFuneral-mainFuneral (1024-1023)	0	90.0000	0.0000	0.0000	6.5 km of 4-7 Ma right-lateral oblique separation (312°) on the fault between these two blocks	(Cemen and Wright, 1990; Applegate and Hodges, 1995)
	4	6.8788	-21.0804	0.0003		
	7	36.1802	6.0580	0.0590		
Bare-mainFuneral (1030-1023)	0	90.0000	0.0000	0.0000	~14 km of 12-7 Ma right-lateral separation (289°) on Amargosa segment Stateline fz based on offset anticline and Eocene-early Miocene rocks	(Wright and Troxel, 1993; Fridrich et al., 2012; Lutz, 2021)
	7	90.0000	0.0000	0.0000		
	12	43.6370	18.9035	0.1270		
Bullfrog-mainFuneral (1029-1023)	0	90.0000	0.0000	0.0000	35 km of 12-7 Ma normal-sense separation (306°) along the Bullfrog Hills detachment. Based on assumption that the Bullfrog Hills and Boundary Canyon detachments are part of the same surface.	(Hamilton, 1988; Maldonado, 1990; Beyene, 2011)
	7	36.2621	74.6176	0.0020		
	12	39.7573	12.0696	0.3164		
Greenwater-swFuneral (1015_1024)	0	90.0000	0.0000	0.0000	9 km 6.5-3.5 Ma dextral separation based on an offset basal conglomerate of the Furnace Creek Formation	(Blair et al., 1999; Fridrich and Thompson, 2011)
	3.5	90.0000	0.0000	0.0000		
	6.5	43.8788	18.4714	0.0721		
mainFuneral-Resting Spring (1023-1025)	0	90.0000	0.0000	0.0000	~22.6 km of 16-7 Ma normal-sense separation (286°) based on thrust belt correlation and cross section reconstruction	Lutz et al., 2021; Fridrich et al., 2012
	7	90.0000	0.0000	0.0000		
	16	50.5202	36.8588	0.2032		
Specter-Spotted (1032-1033)	0	90.0000	0.0000	0.0000	75° of 18-10 Ma CW vertical axis rotation to re-align thrust structures	(Snow and Prave, 1994; Snow and Wernicke, 2000)
	10	90.0000	0.0000	0.0000		
	18	36.9577	115.8616	12.3659		
Spotted-Spring (1033-1041)	0	90.0000	0.0000	0.0000	63° of 18-10 Ma CW vertical axis rotation to re-align thrust structures	(Snow and Prave, 1994; Snow and Wernicke, 2000)
	10	90.0000	0.0000	0.0000		
	18	36.6464	116.0669	62.5470		
Montgomery-Spring (1034-1041)	4	90.0000	0.0000	0.0000	35° of 16-4 Ma CW vertical axis rotation and ~25 km of dextral oblique separation along the West Spring Mtns fault; re-alignment of thrust structures	(Snow and Wernicke, 2000; Lutz et al., 2021)
	16	36.5979	115.6534	35.6415		

Table S3

Euler Pole rotations and kinematic inputs for the southern reconstruction path

Fault Block Restoration	Time (Ma)	Longitude (°)	Latitude (°)	Angle (°)	Kinematic inputs and notes	References
Argus-Slate (1036-1037)	0	90.0000	0.0000	0.0000	7° of 3-0 Ma CW vertical-axis rotation from paleomag and 17.1 km total separation (300°) on Panamint detachment from offset volcanics; setup yields 1 mm/yr post-3 Ma slip rate on Searles Valley fault and 0.3-0.6 mm/yr slip rate on the Ash Hill fault	(Schweig, 1989; Densmore and Anderson, 1997; Walker et al., 2005; Andrew and Walker, 2009)
	3	36.0419	117.2465	7.0000		
	15	38.2727	117.2437	0.5389		
Slate-Panamint1 (1027-1012)	0	90.0000	0.0000	0.0000	17.1 km total separation (300°) on Panamint detachment based on offset volcanics; 14.7 km (296°) of which between Slate Rng and Panamint Mtns	(Walker et al., 2005; Andrew and Walker, 2009)
	4.2	40.6102	11.1556	0.1052		
	15	42.4766	14.2776	0.1305		
Granite/Avawatz-Slate (1038-1037)	0	90.0000	0.0000	0.0000	Total Garlock Fault zone offset of ~64-74 km based on Independence Dike Swarm, East-Sierran thrust system, eugioclinal Pz rocks, basal passive margin sequence, and Miocene volcanics (Dacite domes and Bedrock Spring fm); ~33 km separation since ca. 3.8 Ma on conglomerate of Golden Valley/ Goler Gulch; ~19 km separation from 7-3.8 Ma	(Smith, 1962; Michael, 1966; Smith and Ketner, 1970; Jahns et al., 1971; Davis and Burchfiel, 1973; Carr et al., 1997; Monastero et al., 1997), (Andrew et al., 2014)
	3.8	34.5124	116.7611	16.2392		
	7	34.4442	116.7199	22.1881		
	10.5	34.5566	116.6851	27.7993		

Table S4

Thermo-chronometric data shown in Fig. S3

Mountain Range	Cooling Age (Ma)	Age Type	Reference
White Mountains	11-13 Ma	AFT and (U-Th)/He	(Stockli et al., 2003)
White Mountains	3-4 Ma	Apatite (U-Th)/He	(Stockli et al., 2003)
Inyo Mountains	2.5-3.2 Ma	Apatite (U-Th)/He	(Lee et al., 2009)
Silver Peak Range	11 Ma	ZFT	(Oldow et al., 1994)
Silver Peak Range	6-7 Ma	AFT	(Oldow et al., 1994)
Bare Mountain	10-11 Ma	AFT	(Ferrill et al., 2012)
Funeral Mountains	9-11 Ma	Zircon (U-Th)/He	(Beyene, 2011)
Funeral Mountains	7 Ma	Zircon (U-Th)/He	(Beyene, 2011)
Funeral Mountains	5.5 Ma	AFT	(Holm and Dokka, 1991)
N. Black Mountains	1-4 Ma	Apatite (U-Th)/He	(Sizemore et al., 2019)
Central Black Mtns	4-7 Ma	Zircon (U-Th)/He	(Bidgoli et al., 2015)
S. Black Mountains	8.5-5.4 Ma	Zircon (U-Th)/He	(Bidgoli et al., 2015)
Panamint Range	2.5-4.5 Ma	Apatite (U-Th)/He	(Bidgoli et al., 2015)
McCullough Range	16-11 Ma	Apatite (U-Th)/He	(Mahan et al., 2009)
McCullough Range	5 Ma	Apatite (U-Th)/He	(Mahan et al., 2009)
Slate Range	6-8 Ma	Apatite (U-Th)/He	(Walker et al., 2014)

AFT: apatite fission track. ZFT: zircon fission track

RECONSTRUCTION OF THE DEFLECTIONS IN THE LAB AND MOHO DEPTH GRADIENTS

Both the NW-trending part of the overall NE-trending LAB depth gradient (Figs. 1C main text and S8) and the Moho depth gradient deflections were reconstructed using a simple "cut and slide" method (Fig. S4-S8). We chose a cut line through the center of the whole-lithosphere shear zone (see Fig. 1A in main text), then translated the western slice to the SE along the cut line until the LAB depth gradient and Moho depth-contours were re-aligned. Maximum and minimum dextral offsets were estimated by reconstructing the most and least amount of offset, respectively while still re-aligning the LAB depth gradient and Moho depth contours. Table S5 and Figs. S4-S8 summarize the results of these basic reconstructions.

Table S5

Inferred Moho offsets from reconstruction of ENE-WSW-striking, NNW-SSE-trending crustal thickness gradient

Moho depth/crustal thickness model	Dextral offset magnitude	Notes
Gilbert, 2012 (Fig. S5)	59 ± 14 km	Used ~34 km crustal thickness contour; sharply offset between the FCFZ and SFZ
Tape et al., 2012 (Fig. S6)	56 ± 6 km	Used -36 km Moho depth contour; deflected between the FCFZ and SFZ
	0-10 km	Used -34 km Moho depth contour; little offset between the FCFZ and SFZ; possibly offset along the PVFZ
Shen and Ritzwoller, 2016 (Fig. S7)	70 ± 8 km	Used ~32 km crustal thickness contour; sharply offset between the FCFZ and SFZ
Buehler and Shearer, 2010 (Fig. S8)	65 ± 15 km	Used 28-30 km crustal thickness contours; deflected over broad area between FCFZ and LVSZ
Lee et al., 2014	did not calculate	In W DVR: faults offset velocity structures at 10 km depth, but probably not 20 km depth slice (e.g. HMF) In E DVR: FCFZ and SFZ clearly truncate velocity structures at 10 km and 20 km depth slices

HMF: Hunter Mountain fault zone; LVSZ: Las Vegas Valley shear zone; FCFZ: Furnace Creek fault zone; SFZ: Stateline fault zone

Maps showing reconstruction of the LAB depth gradient deflection

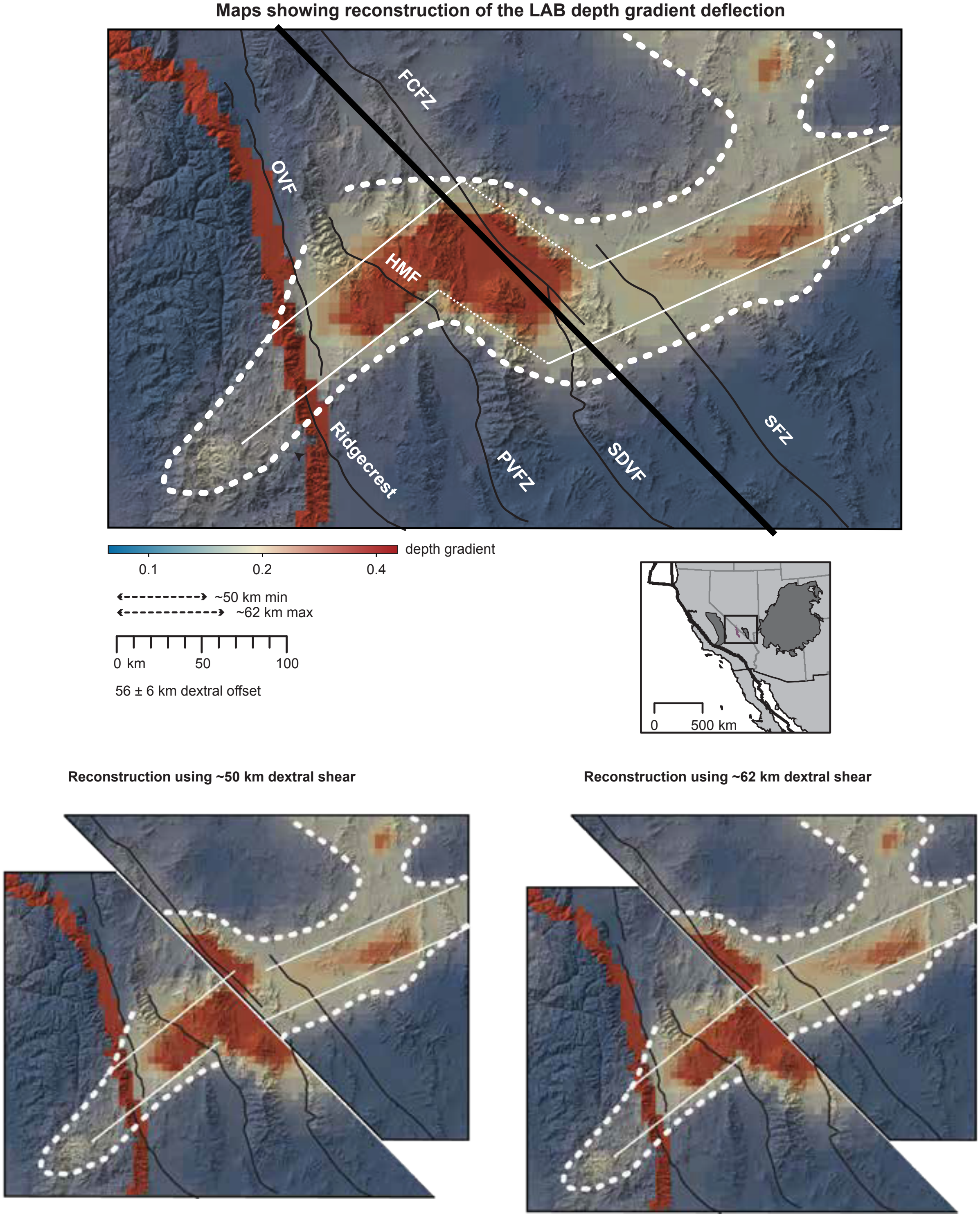

Figure S4. Reconstructions of the dextral deflection in the LAB depth gradient. See Fig. S2 for abbreviations.

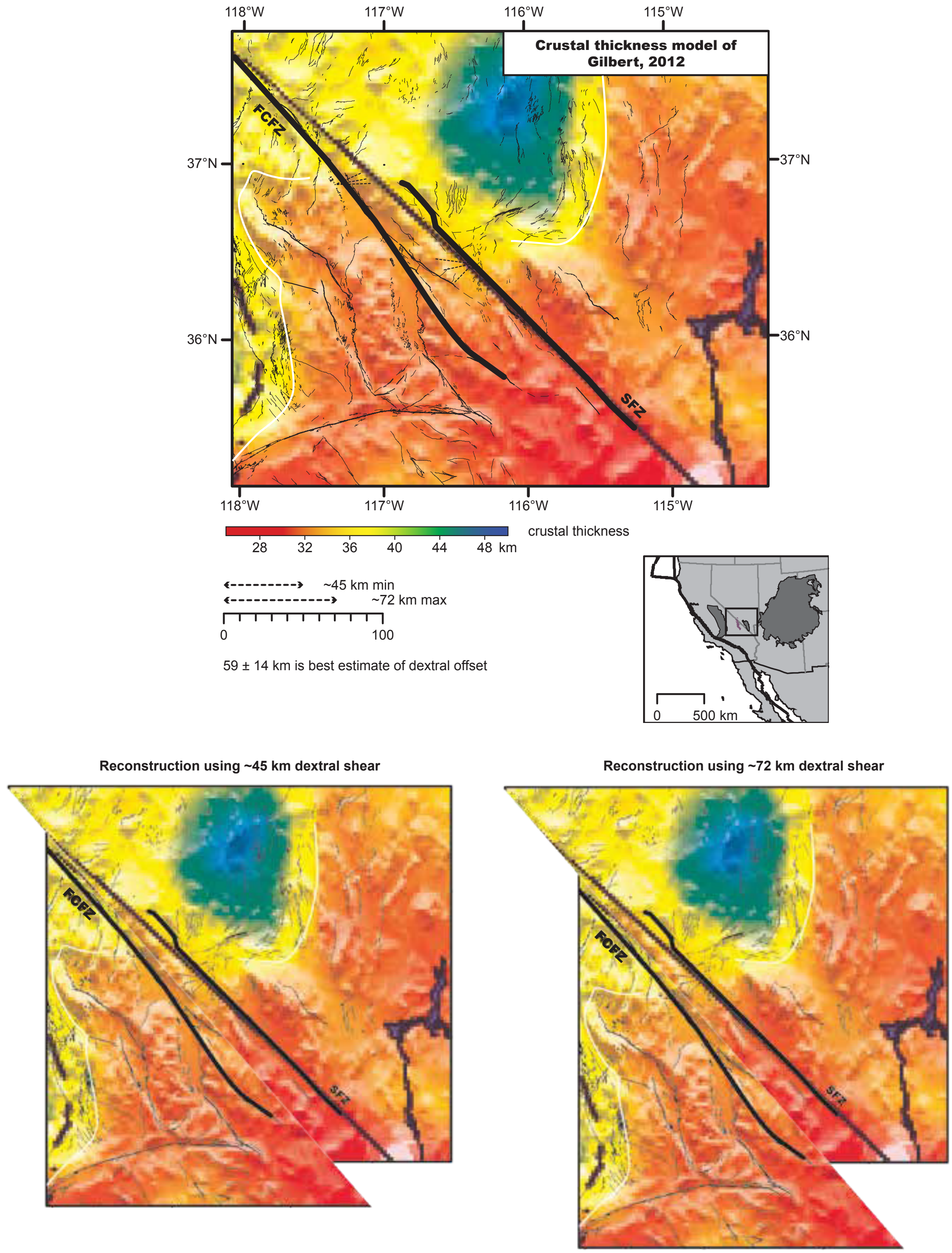

Figure S5. Reconstructions of the dextral deflection in the Moho depth gradient. Map after Gilbert (2012). FCFZ: Furnace Creek fault zone. SFZ: Stateline fault zone.

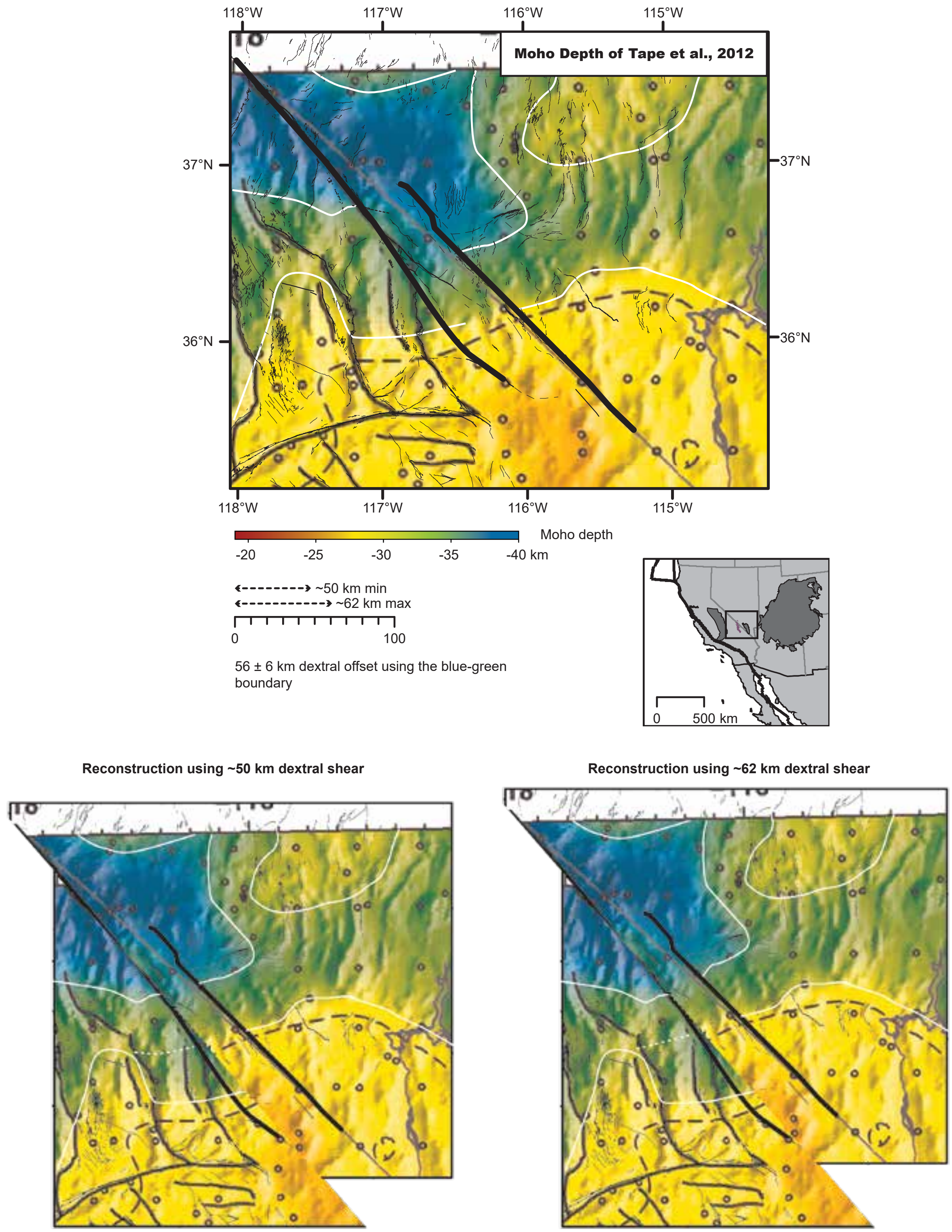

Figure S6. Reconstructions of the dextral deflection in the Moho depth gradient. Map after Tape et al. (2012). FCFZ: Furnace Creek fault zone. SFZ: Stateline fault zone.

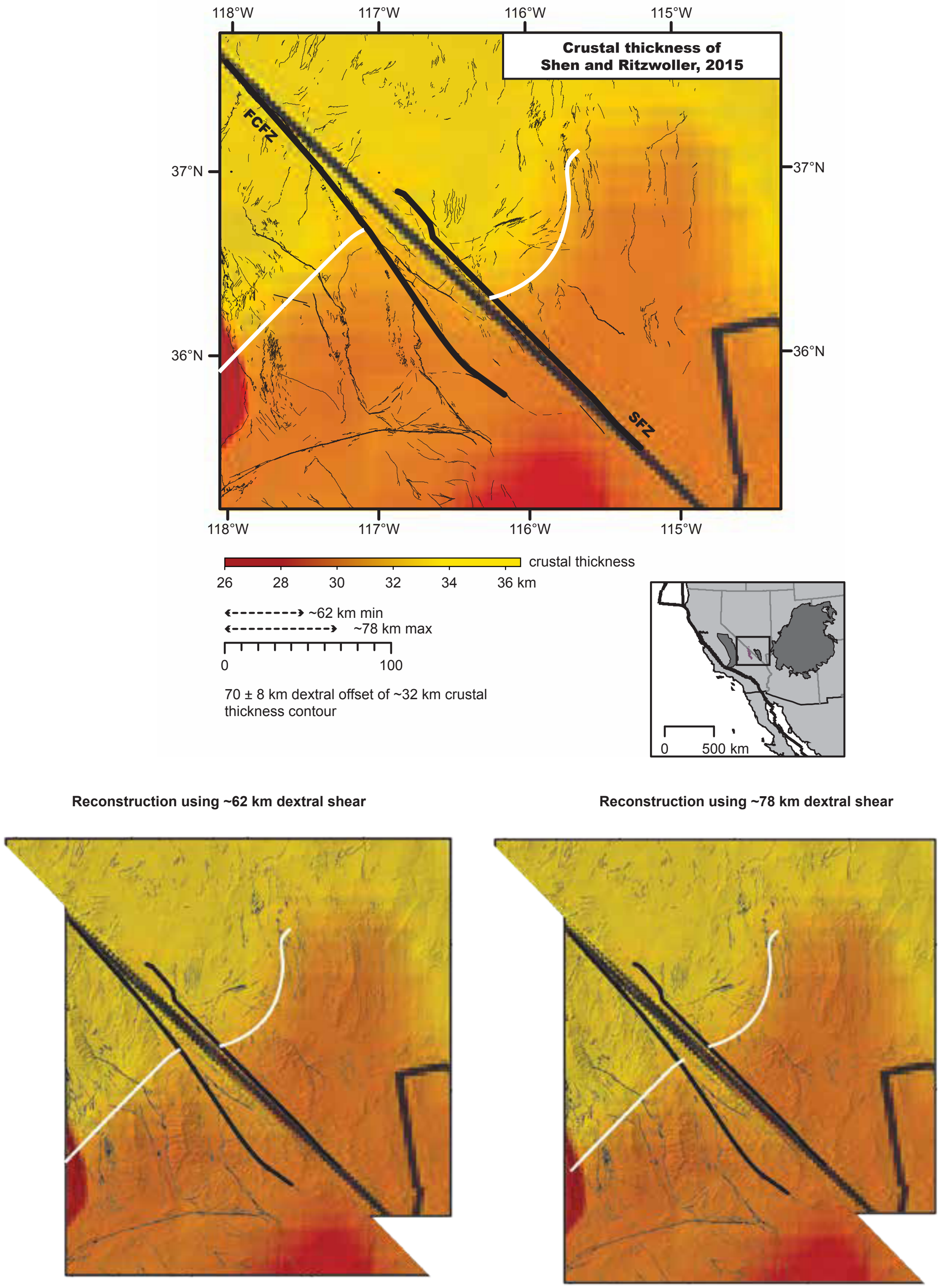

Figure S7. Reconstructions of the dextral deflection in the Moho depth gradient. Map after Shen and Ritzwoller (2016). FCFZ: Furnace Creek fault zone. SFZ: Stateline fault zone.

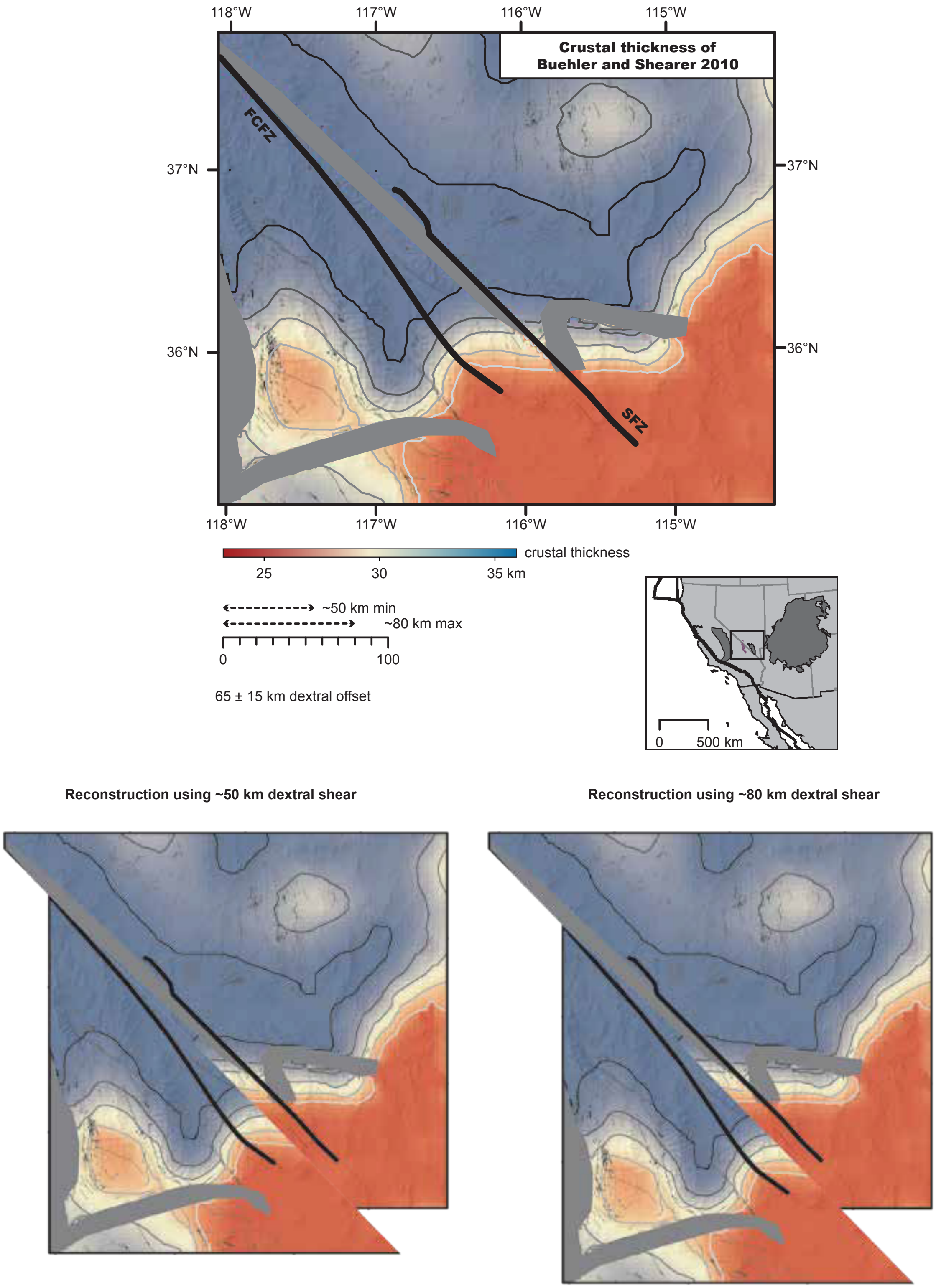

Figure S8. Reconstructions of the dextral deflection in the Moho depth gradient. Map adapted from Buehler and Shearer (2010). FCFZ: Furnace Creek fault zone. SFZ: Stateline fault zone.

UPPER-CRUSTAL DEXTRAL SHEAR MAGNITUDE ACROSS THE WHOLE-LITHOSPHERE SHEAR ZONE

The 57 ± 7 km of upper-crustal dextral shear across the whole-lithosphere shear zone since ca. 8-7 Ma is based on averaging the sum of the total separation of upper-crustal fault blocks across the zone since 8 Ma and 7 Ma, based on kinematic modeling of offset features (see Figs. S2, S9, Animation 1, Table S1, and Lutz, 2021). The post-8 Ma separation along the Fish Lake Valley-Northern Death Valley-Furnace Creek fault zone (abbreviated FCFZ; See Fig. S2) of ~45-48 km was calculated as separation between the White Mountains (block 1004 in GPlates model) and the Funeral Mountains (block 1023 in GPlates model). This was added to the post-8 Ma separation along the Stateline fault zone (SFZ~16 km), which was calculated as separation between the Kingston Range (block 1027 in GPlates model) and the Spring Mountains (block 1041 in GPlates model). Total post-7 Ma separations along the FCFZ and SFZ are ~38 km and ~13 km, respectively. Therefore, the magnitudes of post-8 and post-7 Ma upper-crustal dextral shear across the whole-lithosphere shear zone are 64 km and 50 km, respectively (57 ± 7 km). This magnitude was close to the magnitudes estimated from the LCML offset markers (the deflected or offset depth gradients documented above) and so was considered to be the time-frame for when whole-lithosphere shear initiated.

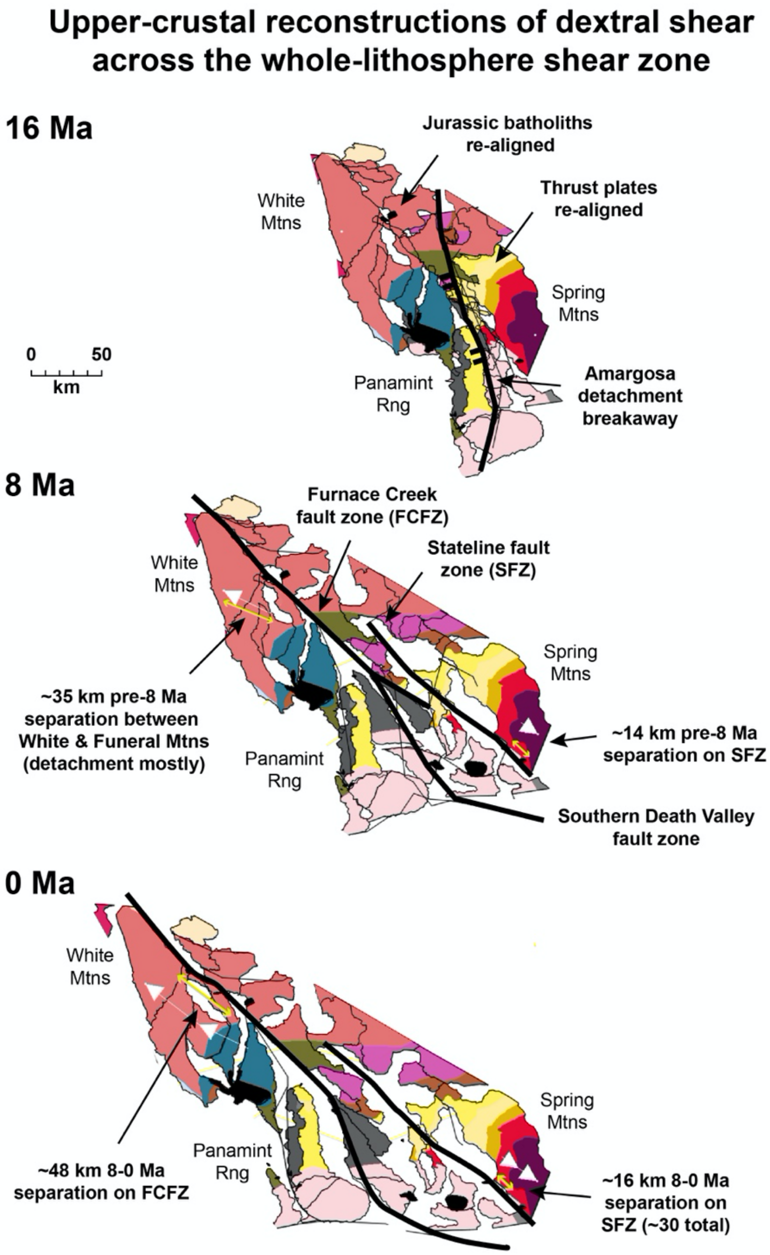

Figure S9. Reconstructions of upper-crustal extension and shear across the whole-lithosphere shear zone. The reconstruction shows the magnitude of separation across the area bounded by the Furnace Creek and Stateline fault zones for pre-8 Ma decoupled conditions and post-8 Ma coupled, whole-lithosphere shear. Specific offset markers are listed in Table 1 and described in detail in Lutz, 2021. See Fig. S2 for the explanation of thrust plates (colored polygons).

SUPPLEMENTAL REFERENCES

Andrew, J.E., and Walker, J.D., 2009, Reconstructing late Cenozoic deformation in central Panamint Valley, California: Evolution of slip partitioning in the Walker Lane: Geosphere, v. 5, no. 3, p. 172–198, doi: 10.1130/GES00178.1.

Andrew, J.E., Walker, J.D., and Monastero, F.C., 2014, Evolution of the central Garlock fault zone, California: A major sinistral fault embedded in a dextral plate margin: GSA Bulletin, v. 127, no. 1-2, p. 227–249, doi: 10.1130/B31027.1.

Applegate, J.D.R., and Hodges, K.V., 1995, Mesozoic and Cenozoic extension recorded by metamorphic rocks in the Funeral Mountains, California: Geological Society of America Bulletin, v. 107, no. 9, p. 1063–1076, doi: 10.1130/0016-7606(1995)107<1063:macerb>2.3.co;2.

Axen, G.J., 1993, Ramp-flat detachment faulting and low-angle normal reactivation of the Tule Springs thrust, southern Nevada: Geological Society of America Bulletin, v. 105, no. 8, p. 1076–1090.

Bachman, S.B., 1978, Pliocene-Pleistocene break-up of the Sierra Nevada–White-Inyo Mountains block and formation of Owens Valley: Geology, v. 6, no. 8, p. 461–463.

Bacon, S.N., and Pezzopane, S.K., 2007, A 25,000-year record of earthquakes on the Owens Valley fault near Lone Pine, California: Implications for recurrence intervals, slip rates, and segmentation models: Geological Society of America Bulletin, v. 119, no. 7-8, p. 823–847.

Beyene, M.A., 2011. Mesozoic burial, Mesozoic and Cenozoic exhumation of the Funeral Mountains core complex, Death Valley, Southeastern California. PhD Thesis; 363 p. University of Nevada, Las Vegas.

Bidgoli, T.S., Amir, E., Walker, J.D., Stockli, D.F., Andrew, J.E., and Caskey, S.J., 2015, Low-temperature thermochronology of the Black and Panamint mountains, Death Valley, California: Implications for geodynamic controls on Cenozoic intraplate strain: Lithosphere, v. 7, no. 4, p. 473–480, doi: 10.1130/L406.1.

Blair, T.C., Raynolds, R.G., Wright, L.A., and Troxel, B.W., 1999, Sedimentology and tectonic implications of the Neogene synrift Hole in the Wall and Wall Front members, Furnace Creek basin, Death Valley, *in* Wright, L.A. and Troxel, B.W. eds., *Cenozoic basins of the Death Valley Region: Geological Society of America Special Paper 333*, p. 127-168.

Blakely, R.J., Jachens, R.C., Calzia, J.P., and Langenheim, V.E., 1999, Cenozoic basins of the Death Valley extended terrane as reflected in regional-scale gravity anomalies, *in* Wright, L.A. and Troxel, B.W. eds., *Cenozoic basins of the Death Valley Region: Geological Society of America Special Paper 333*, p. 1-16.

Burchfiel, B.C., Hamill, G.S., and Wilhelms, D.E., 1983, Structural geology of the Montgomery Mountains and the northern half of the Nopah and Resting Spring Ranges, Nevada and California: Geological Society of America Bulletin, v. 94, no. 11, p. 1359.

Burchfiel, B.C., Hodges, K.V., and Royden, L.H., 1987, Geology of Panamint Valley-Saline Valley pull-apart system, California: Palinspastic evidence for low-angle geometry of a Neogene range-bounding fault: Journal of Geophysical Research: Solid Earth, v. 92, no. B10, p. 10422–10426.

Carr, M.D., Christiansen, R.L., Poole, F.G., and Goodge, J.W., 1997, Bedrock geologic map of the El Paso Mountains in the Garlock and El Paso Peaks 7–1/2′ quadrangles: Kern County, California: US Geological Survey Miscellaneous Investigations Series Map I-2389.

Cemen, I., and Wright, L.A., 1990, Effect of Cenozoic extension on Mesozoic thrust surfaces, *in*, Wernicke, B.P., ed., *Basin and Range Extensional Tectonics Near the Latitude of Las Vegas, Nevada,* Geological Society of America Memoir 176, p. 305-316.

Davis, G.A., and Burchfiel, B.C., 1973, Garlock fault: An intracontinental transform structure, southern California: Geological Society of America Bulletin, v. 84, no. 4, p. 1407–1422.

Davis, G.A., Fowler, T.K., Bishop, K.M., Brudos, T.C., Friedmann, S.J., Burbank, D.W., Parke, M.A., and Burchfiel, B.C., 1993, Pluton pinning of an active Miocene detachment fault system, eastern Mojave Desert, California: Geology, v. 21, no. 7, p. 627–5.

Densmore, A.L., and Anderson, R.S., 1997, Tectonic geomorphology of the Ash Hill fault, Panamint Valley, California: Basin Research, v. 9, no. 1, p. 53–63.

Duebendorfer, E.M., and Black, R.A., 1992, Kinematic role of transverse structures in continental extension: An example from the Las Vegas Valley shear zone, Nevada: Geology, v. 20, no. 12, p. 1107–1110.

Duebendorfer, E.M., Beard, L.S., and Smith, E.I., 1998, Restoration of Tertiary deformation in the Lake Mead region, southern Nevada: The role of strike-slip transfer faults: Accommodation zones and transfer zones: The regional segmentation of the Basin and Range province: Geological Society of America Special Paper, v. 323, p. 127–148.

Ferrill, D.A., Morris, A.P., Stamatakos, J.A., Waiting, D.J., Donelick, R.A., and Blythe, A.E., 2012, Constraints on exhumation and extensional faulting in southwestern Nevada and eastern California, U.S.A., from zircon and apatite thermochronology: Lithosphere, v. 4, no. 1, p. 63–76, doi: 10.1130/L171.1.

Flemming, 2018, Geometry, timing, and kinematics of Neogene extensional and transtensional structures of southern Death Valley: Implications for regional reconstructions and a corrective method for rigid body rotations. [PHD Thesis]. The University of Texas, El Paso.

Foy, T.A., Frankel, K.L., Lifton, Z.M., Johnson, C.W., and Caffee, M.W., 2012, Distributed extensional deformation in a zone of right-lateral shear: Implications for geodetic versus geologic rates of deformation in the eastern California shear zone-Walker Lane: Tectonics, v. 31, no. 4, doi: 10.1029/2011TC002930.

Frankel, K.L., Dolan, J.F., Finkel, R.C., Owen, L.A., and Hoeft, J.S., 2007, Spatial variations in slip rate along the Death Valley-Fish Lake Valley fault system determined from LiDAR topographic data and cosmogenic 10Be geochronology: v. 34, no. 18, doi: 10.1029/2007GL030549.

Fridrich, C.J., and Thompson, R.A., 2011, Cenozoic tectonic reorganizations of the Death Valley region, southeast California and southwest Nevada. U.S. Geological Survey Professional Paper 1783. 36 p.

Fridrich, C.J., Thompson, R.A., Slate, J.L., Berry, M.E., and Machette, M.N., 2012, Geologic map of the southern Funeral Mountains including nearby groundwater discharge sites in Death Valley National Park, California and Nevada: Scientific Investigations Map, no. 3151, doi: 10.3133/sim3151.

Guest, B., Niemi, N., 1996, Clayton, R., Ducea, M., Jones, C.H., Mahan, K.H., and Niemi, N.A., 2007, Stateline fault system: A new component of the Miocene-Quaternary Eastern California shear zone: Geological Society of America Bulletin, v. 119, no. 11-12, p. 1337–1347.

Guest, B., Pavlis, T.L., Golding, H., and Serpa, L., 2003, Chasing the Garlock: A study of tectonic response to vertical axis rotation: Geology, v. 31, no. 6, p. 553-556.

Hall, W.E., 1971, Geology of the Panamint Butte Quadrangle, Inyo County, California: U.S. Geological Survey Bulletin, no. 1299, 67 p.

Hamilton, W.B., 1988, Detachment faulting in the Death Valley region, California and Nevada: Geologic and hydrologic investigations of a potential nuclear waste disposal site at Yucca Mountain, southern Nevada US Geological Survey Bulletin, v. 1790, p. 51–85.

Hill, E.M., and Blewitt, G., 2006, Testing for fault activity at Yucca Mountain, Nevada, using independent GPS results from the BARGEN network, Geophyscial Research Letters, v. 33, no. 14, p. 1008–1005, doi: 10.1029/2006GL026140.

Hodges, K.V., McKenna, L.W., Stock, J., Knapp, J., Page, L., Sternlof, K., Silverberg, D., Wüst, G., and Walker, J.D., 1989, Evolution of extensional basins and basin and range topography west of Death Valley, California: Tectonics: v. 8, no. 3, p. 453–467, doi: 10.1029/tc008i003p00453.

Hoeft, J.S., and Frankel, K.L., 2010, Temporal variations in extension rate on the Lone Mountain fault and strain distribution in the eastern California shear zone–Walker Lane: Geosphere, v. 6, no. 6, p. 917–936, doi: 10.1130/GES00603.1.

Hoisch, T.D., and Simpson, C., 1993, Rise and tilt of metamorphic rocks in the lower plate of a detachment fault in the Funeral Mountains, Death Valley, California: Journal of Geophysical Research: Solid Earth, v. 98, no. B4, p. 6805–6827, doi: 10.1029/92jb02411.

Holm, D.K., and Dokka, R.K., 1991, Major Late Miocene cooling of the middle crust associated with extensional orogenesis in the Funeral Mountains, California: v. 18, no. 9, p. 1775–1778, doi: 10.1029/91gl02079.

Jahns, R.H., Troxel, B.W., and Wright, L.A., 1971, Some structural implications of a late Precambrian–Cambrian section in the Avawatz Mountains, California. Geological Society of America Abstracts with Programs v. 3, p. 140.

Kirby, E., Anandakrishnan, S., Phillips, F., and Marrero, S., 2008, Late Pleistocene slip rate along the Owens Valley fault, eastern California: Geophysical Research Letters, v. 35, no. 1.

Klinger, R.E., and Sarna-Wojcicki, A.M., 2001, Stop A2 Active tectonics and deposition in the Lake Rogers basin: Quaternary and Late Pliocene Geology of the Death Valley Region: Recent Observations on Tectonics, Stratigraphy, and Lake Cycles (Guidebook for the 2001 Pacific Cell—Friends of the Pleistocene Fieldtrip), p. 25.

Knott, J.R., Lutz, B.M., Heizler, M., Phillips, F.M., and Heitkamp, K., 2019, Tectonic Reorganization in the Death Valley Area at 4 Ma: Geological Society of America Abstracts with Programs. V. 51, no. 5.

Lee, J., Rubin, C.M., and Calvert, A., 2001a, Quaternary faulting history along the Deep Springs fault, California: Geological Society of America Bulletin, v. 113, no. 7, p. 855–869.

Lee, J., Spencer, J., and Owen, L., 2001b, Holocene slip rates along the Owens Valley fault, California: Implications for the recent evolution of the Eastern California Shear Zone: Geology, v. 29, no. 9, p. 819–822.

Lee, J., Stockli, D.F., Owen, L.A., Finkel, R.C., and Kislitsyn, R., 2009, Exhumation of the Inyo Mountains, California: Implications for the timing of extension along the western boundary of the Basin and Range Province and distribution of dextral fault slip rates across the eastern California shear zone: Tectonics, v. 28, no. 1, p. n/a–n/a, doi: 10.1029/2008TC002295.

Lifton, Z.M., Frankel, K.L., and Newman, A.V., 2015, Latest Pleistocene and Holocene slip rates on the Lone Mountain fault: Evidence for accelerating slip in the Silver Peak-Lone Mountain extensional complex: Tectonics, v. 34, no. 3, p. 449–463, doi: 10.1002/2013TC003512.

Luckow, H., Pavlis, T., Serpa, L., Guest, B., Wagner, D., Snee, L., Hensley, T., Korjenkov, A., 2005. Late Cenozoic sedimentation and volcanism during transtensional deformation in Wingate Wash and the Owlshead Mountains, Death Valley, Earth-Science Reviews, v. 73, p. 177–219, doi:10.1016/j.earscirev.2005.07.013

Machette M. Haller K. Wald L. (2004). Quaternary Fault and Fold Database for the nation, USGS Fact Sheet FS2004-3033 , 2 p.

Mahan, K.H., Guest, B., Wernicke, B.P., and Niemi, N.A., 2009, Low-temperature thermochronologic constraints on the kinematic history and spatial extent of the Eastern California shear zone: Geosphere, v. 5, no. 6, p. 483–495, doi: 10.1130/GES00226.1.

Maldonado, F., 1990, Structural geology of the upper plate of the Bullfrog Hills detachment fault system, southern Nevada: Geological Society of America Bulletin, v. 102, no. 7, p. 992–1006.

Michael, E.D., 1966, Large lateral displacement on Garlock fault, California, as measured from offset fault system: Geological Society of America Bulletin, v. 77, no. 1, p. 111–114.

Monastero, F.C., Sabin, A.E., and Walker, J.D., 1997, Evidence for post-early Miocene initiation of movement on the Garlock fault from offset of the Cudahy Camp Formation, east-central California: Geology, v. 25, no. 3, p. 247–250.

Mueller, N.J., 2019, Pliocene Kinematic Reorganization, Fault Geometry, Basin Evolution, and Displacement Budget Along the Furnace Creek – Fish Lake Valley Fault Zone, Eastern California and Western Nevada:, p. 1–170.

Nachbor, A.C., and Wetmore, P., 2017, Preliminary Structure from motion data for the Towne Pass fault, northern Death Valley National Park, California, Geological Society of America Abstracts with programs, v. 49, no. 6, doi: 10.1130/abs/2017AM-302776

Niemi, N.A., Wernicke, B.P., Brady, R.J., Saleeby, J.B., and Dunne, G.C., 2001, Distribution and provenance of the middle Miocene Eagle Mountain Formation, and implications for regional kinematic analysis of the Basin and Range province: Geological Society of America Bulletin, v. 113, no. 4, p. 419–442.

Oakes, E.H., 1987, Age and rates of displacement along the Furnace Creek fault zone, northern Death Valley, California: Geological Society of America Abstracts with Programs. v. 19, p. 437.

Oldow, J.S., Elias, E.A., Ferranti, L., McClelland, W.C., McIntosh, W.C., and Cashman, P.H., 2009, Late Miocene to Pliocene synextensional deposition in fault-bounded basins within the upper plate of the western Silver Peak–Lone Mountain extensional complex, west-central Nevada: Late Cenozoic structure and evolution of the Great Basin–Sierra Nevada transition: Geological Society of America Special Paper, v. 447, p. 275–312.

Oldow, J.S., Kohler, G., and Donelick, R.A., 1994, Late Cenozoic extensional transfer in the Walker Lane strike-slip belt, Nevada: Geology, v. 22, no. 7, p. 637-640.

Oswald, J.A., and Wesnousky, S.G., 2002, Neotectonics and Quaternary geology of the Hunter Mountain fault zone and Saline Valley region, southeastern California: Geomorphology, v. 42, no. 3, p. 255–278, doi: 10.1016/S0169-555X(01)00089-7.

Petronis, M.S., Geissman, J.W., Holm, D.K., Wernicke, B.P., and Schauble, E., 2002a, Assessing vertical axis rotations in large-magnitude extensional settings: A transect across the Death Valley extended terrane, California: Journal of Geophysical Research: Solid Earth, v. 107, no. B1, p. EPM 4–1–EPM 4–21, doi: 10.1029/2001JB000239.

Petronis, M.S., Geissman, J.W., Oldow, J.S., and McIntosh, W.C., 2002b, Paleomagnetic and 40Ar/39Ar geochronologic data bearing on the structural evolution of the Silver Peak extensional complex, west-central Nevada: Geological Society of America Bulletin, v. 114, no. 9, p. 1108–1130.

Petronis, M.S., Geissman, J.W., Oldow, J.S., McIntosh, W.C., and Cashman, P.H., 2009, Late Miocene to Pliocene vertical-axis rotation attending development of the Silver Peak–Lone Mountain displacement transfer zone, west-central Nevada: Late Cenozoic structure and evolution of the Great Basin–Sierra Nevada transition: Geological Society of America Special Paper, v. 447, p. 215–253.

Petronis, M.S., Geissman, J.W., Oldow, J.S., McIntosh, W.C., and Roeske, S.M., 2007, Tectonism of the southern Silver Peak Range: Paleomagnetic and geochronologic data bearing on the Neogene development of a regional extensional complex, central Walker Lane, Nevada: Special Papers-Geological Society of America, v. 434, p. 81.

Reheis, M.C., and Sawyer, T.L., 1997, Late Cenozoic history and slip rates of the Fish Lake valley, Emigrant Peak, and Deep Springs fault zones, Nevada and California: Geological Society of America Bulletin, v. 109, no. 3, p. 280–299.

Renik, B., 2010, Distribution of Neogene extension and strike slip in the Death Valley region, California-Nevada, with implications for palinspastic reconstruction and models of normal faulting [Ph.D. thesis]: New York City, Columbia University, 238 p.

Renik, B., and Christie-Blick, N., 2013, A new hypothesis for the amount and distribution of dextral displacement along the Fish Lake Valley-northern Death Valley-Furnace Creek fault zone, California-Nevada: Tectonics, v. 32, no. 2, p. 123–145, doi: 10.1029/2012TC003170.

Schweig, E.S., III, 1989, Basin-range tectonics in the Darwin Plateau, southwestern Great Basin, California: Geological Society of America Bulletin, v. 101, no. 5, p. 652–662, doi: 10.1130/0016-7606(1989)101<0652:brtitd>2.3.co;2.

Smith, G.I., 1962, Large Lateral Displacement on Garlock Fault, Califonia, as Measured from Offset Dike Swarm: AAPG Bulletin, v. 46, no. 1, p. 85–104.

Smith, G.I., and Ketner, K.B., 1970, Lateral displacement on the Garlock fault, southeastern California, suggested by offset sections of similar metasedimentary rocks: US Geological Survey Professional Paper, v. 700, p. D1–D9.

Snow, J.K., and Prave, A.R., 1994, Covariance of structural and stratigraphic trends: Evidence for anticlockwise rotation within the Walker Lane Belt Death Valley region, California and Nevada: Tectonics, v. 13, no. 3, p. 712–724.

Snow, J.K., and Wernicke, B.P., 2000, Cenozoic tectonism in the central Basin and Range; magnitude, rate, and distribution of upper crustal strain: American Journal of Science, v. 300, no. 9, p. 659–719, doi: 10.2475/ajs.300.9.659.

Snow, J.K., and White, C., 1990, Listric normal faulting and synorogenic sedimentation, northern Cottonwood Mountains, Death Valley region, California, *in*, Wernicke, B.P., *Basin and Range Extensional Tectonics Near the Latitude of Las Vegas, Nevada:* Geological Society of America Memoir, v. 176, p. 413–445.

Snyder, N.P., and Hodges, K.V., 2000, Depositional and tectonic evolution of a supradetachment basin: 40Ar/39Ar geochronology of the Nova Formation, Panamint Range, California: Basin Research, v. 12, no. 1, p. 19–30, doi: 10.1046/j.1365-2117.2000.00108.x.

Sternloff, K.R., 1988, Structural style and kinematic history of the active Panamint-Saline extensional system, Inyo county, California [Ph.D. thesis]: Cambridge, Massachusetts Institute of Technology, 30 p

Stewart, J.H., 1983, Extensional tectonics in the Death Valley area, California: Transport of the Panamint Range structural block 80 km northwestward: Geology, v. 11, no. 3, p. 153, doi: 10.1130/0091-7613(1983)11<153:etitdv>2.0.co;2.

Stewart, J.H., and Diamond, D.S., 1990, Changing patterns of extensional tectonics; overprinting of the basin of the middle and upper Miocene Esmeralda Formation in western Nevada by younger structural basins, *in* Wernicke, B.P. ed., *Basin and Range Extensional Tectonics Near the Latitude of Las Vegas, Nevada,* Geological Society of America Memoir, p. 447–476.

Stockli, D.F., Dumitru, T.A., McWilliams, M.O., and Farley, K.A., 2003, Cenozoic tectonic evolution of the White Mountains, California and Nevada: Geological Society of America Bulletin, v. 115, no. 7, p. 788–816, doi: 10.1130/0016-7606(2003)115<0788:cteotw>2.0.co;2.

Topping, D.J., 1993, Paleogeographic reconstruction of the Death Valley extended region: Evidence from Miocene large rock-avalanche deposits in the Amargosa Chaos Basin, California: Geological Society of America Bulletin, v. 105, no. 9, p. 1190–1213, doi: 10.1130/0016-7606(1993)105<1190:protdv>2.3.co;2.

Walker, J.D., Bidgoli, T.S., Didericksen, B.D., Stockli, D.F., and Andrew, J.E., 2014, Middle Miocene to recent exhumation of the Slate Range, eastern California, and implications for the timing of extension and the transition to transtension: Geosphere, v. 10, no. 2, p. 276–291, doi: 10.1130/ges00947.1.

Walker, J.D., Kirby, E., and Andrew, J.E., 2005, Strain transfer and partitioning between the Panamint Valley, Searles Valley, and Ash Hill fault zones, California: Geosphere, v. 1, no. 3, p. 111, doi: 10.1130/GES00014.1.

Wernicke, B.P., 2004, Tectonic implications of a dense continuous GPS velocity field at Yucca Mountain, Nevada: Journal of Geophysical Research: Solid Earth, v. 109, no. B12, p. 189, doi: 10.1029/2003JB002832.

Wernicke, B.P., Axen, G.J., and Snow, J.K., 1988, Basin and Range extensional tectonics at the latitude of Las Vegas, Nevada: Geological Society of America Bulletin, v. 100, no. 11, p. 1738–1757.

Wright, L.A., and Troxel, B.W., 1993, Geologic map of the central and northern Funeral Mountains and adjacent areas: Death Valley region, southern California: US Geological Survey Miscellaneous Investigations Series Map I–2305.